



OPEN

## ABCA1 deficiency contributes to podocyte pyroptosis priming via the APE1/IRF1 axis in diabetic kidney disease

Marie Ito<sup>1,2✉</sup>, Gloria Michelle Ducasa<sup>1</sup>, Judith David Molina<sup>1</sup>, Javier Varona Santos<sup>1</sup>, Shamroop Kumar Mallela<sup>1</sup>, Jin Ju Kim<sup>1</sup>, Mengyuan Ge<sup>1</sup>, Alla Mitrofanova<sup>1</sup>, Alexis Sloan<sup>1</sup>, Sandra Merscher<sup>1</sup>, Imari Mimura<sup>2</sup> & Alessia Fornoni<sup>1✉</sup>

Decreased ATP Binding Cassette Transporter A1 (ABCA1) expression and caspase-4-mediated noncanonical inflammasome contribution have been described in podocytes in diabetic kidney disease (DKD). To investigate a link between these pathways, we evaluated pyroptosis-related mediators in human podocytes with stable knockdown of ABCA1 (siABCA1) and found that mRNA levels of IRF1, caspase-4, GSDMD, caspase-1 and IL1 $\beta$  were significantly increased in siABCA1 compared to control podocytes and that protein levels of caspase-4, GSDMD and IL1 $\beta$  were equally increased. IRF1 knockdown in siABCA1 podocytes prevented increases in caspase-4, GSDMD and IL1 $\beta$ . Whereas TLR4 inhibition did not decrease mRNA levels of IRF1 and caspase-4, APE1 protein expression increased in siABCA1 podocytes and an APE1 redox inhibitor abrogated siABCA1-induced expression of IRF1 and caspase-4. RELA knockdown also offset the pyroptosis priming, but ChIP did not demonstrate increased binding of NF $\kappa$ B to IRF1 promoter in siABCA1 podocytes. Finally, the APE1/IRF1/Casp1 axis was investigated in vivo. APE1 IF staining and mRNA levels of IRF1 and caspase 11 were increased in glomeruli of BTBR ob/ob compared to wildtype. In conclusion, ABCA1 deficiency in podocytes caused APE1 accumulation, which reduces transcription factors to increase the expression of IRF1 and IRF1 target inflammasome-related genes, leading to pyroptosis priming.

Diabetic kidney disease (DKD) is the one of the main causes of end-stage kidney disease and among the top ten causes of death globally<sup>1</sup>. It also constitutes an independent risk factor of mortality and cardiovascular events in patients with diabetes<sup>2</sup>. Podocytes, which are terminally differentiated epithelial cells with low ability of self-renewal or proliferation, are key constituents of the glomerular filtration barrier. Clinical and experimental data suggest that podocyte loss correlates with the development of albuminuria, indicating the importance of podocyte injury in DKD<sup>3,4</sup>.

We previously demonstrated decreased ATP-binding cassette A1 (ABCA1) expression in glomerular transcripts from patients with DKD and in human podocytes exposed to sera from patients with DKD when compared to patients with diabetes and without DKD. Podocyte-specific Abca1 KO mice were sensitized to DKD injury, and both genetic and pharmacological induction of ABCA1 ameliorated DKD<sup>5,6</sup>. While the primary function of ABCA1 has been largely recognized as a cholesterol/phospholipid exporter, it has become clear that ABCA1 also exports reduction–oxidation factor 1 (Ref-1)/Apurinic/aprimidinic endonuclease 1 (APE1), a transcription factor reducer and AP endonuclease<sup>7</sup>.

Pyroptosis, a form of inflammatory cell death, was found to contribute to podocyte loss in DKD with the main focus on canonical pyroptosis<sup>8</sup>. Pyroptosis requires two steps: priming and activation of the inflammasome. The priming step, in which the inflammasome components are transcriptionally upregulated, allows for the subsequent activation of inflammasome. In canonical pyroptosis, this transcriptional upregulation is induced through the binding of pathogen- and damage-associated molecular patterns (PAMPs and DAMPs) to pattern recognition receptors (PRRs) such as Toll-like receptors (TLRs) or through cytokines such as tumor necrosis factor (TNF)

<sup>1</sup>Department of Medicine, Katz Family Division of Nephrology and Hypertension, Peggy and Harold Katz Family Drug Discovery Center, University of Miami, Miller School of Medicine, University of Miami, Miami, FL 33136, USA. <sup>2</sup>Division of Nephrology and Endocrinology, The University of Tokyo Graduate School of Medicine, Tokyo, Japan. ✉email: marieitou@gmail.com; afornoni@med.miami.edu

and IL1 $\beta$ , thus leading to NF $\kappa$ B activation<sup>9</sup>. Non-canonical pyroptosis is initiated by caspase-4/5 in human or caspase-11 in mice, and eventually causes downstream canonical inflammasome formation<sup>10</sup>. Non-canonical pyroptosis was recently found to mediate podocyte injury in DKD<sup>11</sup>. The main inducers of non-canonical pyroptosis known today are lipopolysaccharide (LPS) and activation of TLR4 signaling<sup>9</sup>. Indeed, activation of TLR4 signaling was shown to enhance pyroptosis in tubular cells in experimental DKD<sup>12</sup>. However, the mechanisms leading to non-canonical pyroptosis priming in podocytes remain unclear.

In this study, we demonstrate that ABCA1 deficiency in DKD contributes to the increase in non-canonical pyroptosis-related genes such as caspase-4/11, gasdermin D, caspase-1 and IL1 $\beta$  but not NLRP3. We also show that ABCA1 deficiency-induced priming of non-canonical pyroptosis is mediated by accumulated APE1, subsequent activation of transcription factors via reduction by APE1 and the enhancement of IRF1 transcription. Therefore, we propose the ABCA1/APE1/IRF1 axis to be a novel inducer of non-canonical pyroptosis in DKD.

## Results

**Non-canonical pyroptosis-related genes are upregulated in ABCA1 KD podocytes.** We previously described that decreased ABCA1 expression in podocytes precedes podocyte injury in DKD and sensitizes podocytes to it<sup>5,6</sup>. Pyroptosis was recently identified as a novel mechanism of podocyte injury in DKD. However, the link between ABCA1 deficiency and pyroptosis has not been investigated<sup>8</sup>. To examine whether ABCA1 deficiency contributes to pyroptosis in podocytes, we measured mRNA levels of genes involved in pyroptosis in ABCA1 knockdown podocytes (siABCA1). mRNA expression of caspase-4, GSDMD, caspase-1 and IL1 $\beta$  was significantly increased in siABCA1 podocytes compared to control ( $p=0.005$  for caspase-4, 0.004 for GSDMD, 0.008 for caspase-1 and 0.01 for IL1 $\beta$ ), whereas NLR family pyrin domain-containing protein 3 (NLRP3) expression decreased (Fig. 1a), in contrast to the previous reports indicating that NLRP3 expression is increased in podocytes treated with high glucose and in experimental DKD<sup>8,13</sup>. At the protein level, caspase-4 and GSDMD were significantly increased in siABCA1 compared to siCO podocytes ( $p=0.007$  for pro caspase-4 and 0.0001 for FL-GSDMD), while caspase-1 expression was increased but at a level that did not reach statistical significance ( $p=0.08$ ) (Fig. 1b). Although IL1 $\beta$  protein in cell lysates did not increase in siABCA1, we found increased IL1 $\beta$  precursor in the supernatants of siABCA1 podocytes when compared to siCO (Fig. 1c). Caspase-4 and GSDMD also increased and caspase-1 had the tendency to increase in their non-cleaved inactive forms in siABCA1 podocytes (Fig. 1a,b). These data demonstrated that ABCA1 knockdown in podocytes primes cells for non-canonical pyroptosis but is not sufficient to activate pyroptosis, which is consistent with our previous observation that ABCA1 deficiency contributes to DKD progression but is not sufficient to cause podocyte injury by itself<sup>6</sup>.

**Non-canonical pyroptosis activation induced by LPS electroporation is enhanced in ABCA1 KD podocytes.** Next, we investigated whether the upregulation of pyroptosis-related genes in ABCA1 KD podocytes contributes to non-canonical pyroptosis activation. Caspase-4 and GSDMD is cleaved and excreted into medium by LPS electroporation, which is compatible with previous reports demonstrating non-canonical pyroptosis activation by LPS electroporation<sup>14,15</sup>. Pan-caspase inhibitor zVAD-fmk reverses the cleavage (Fig. 2a,b). ABCA1 KD significantly enhanced the cleavage ( $p=0.002$  for cleaved caspase-4 (32 kD), 0.0001 for cleaved caspase-4 (40 kD) and 0.0009 for N terminal-GSDMD (N-GSDMD)).

**IRF1 orchestrates the upregulation of non-canonical pyroptosis-related genes in ABCA1 KD podocytes.** Interferon regulatory factor 1 and 2 (IRF1 and 2) are the transcription factors which regulate non-canonical pyroptosis with cell-type specific target genes. For example, in human U937 cells, IRF2 regulates caspase-4 and -1 but not GSDMD and in human EA.hy926 hybrid endothelial cells IRF2 regulates GSDMD but not caspase-4 nor -1<sup>16,17</sup>. IRF1 compensates for IRF2 deficiency<sup>18</sup>. To explore whether IRF1 or 2 plays a role in regulating non-canonical pyroptosis-related genes in siABCA1 podocytes, we conducted qPCR for IRF1 and 2 gene expression in siABCA1 podocytes. Whereas the expression of IRF2 augmented significantly with larger  $n$  but to a small extent in siABCA1 podocytes (siABCA1/siCO ratio:  $1.191 \pm 0.0699$ ,  $p=0.02$ ,  $N=6$ ), that of IRF1 were substantially increased (siABCA1/siCO ratio:  $3.052 \pm 0.4136$ ,  $p=0.002$ ,  $N=3$ ) (Fig. 3a). In order to establish if IRF1 mediates the association between ABCA1 deficiency and pyroptosis, we next investigated whether siRNA knockdown for IRF1 in siABCA1 podocytes would offset the ABCA1 knockdown-induced changes in gene expression. We found mRNA levels of caspase-4, GSDMD and IL1 $\beta$  were significantly decreased in siIRF1 in siABCA1 podocytes ( $p=0.005$  for caspase-4, 0.002 for GSDMD,  $<0.0001$  for IL1 $\beta$ ) while those of caspase-1 were not affected (Fig. 3b). Thus, we concluded that increased IRF1 is responsible for the upregulation of caspase-4, GSDMD and IL1 $\beta$  in siABCA1 podocytes.

**TLR4 does not mediate IRF1 upregulation in ABCA1 KD podocytes.** TLR4 signaling contributes to non-canonical pyroptosis priming<sup>9</sup>. ABCA1 deficiency in macrophages was found to enhance TLRs signaling by increasing TLRs (including TLR4) trafficking to plasma membrane lipid rafts<sup>12,19</sup>. To explore whether TLR4 signaling contributes to IRF1 and its downstream gene expression changes we observed in siABCA1 podocytes, we treated podocytes with TAK-242, a TLR4 inhibitor. The mRNA levels of IRF1 and caspase-4 were not significantly influenced by the inhibition of TLR4 (Fig. 4). These data suggest that TLR4 signaling does not contribute to ABCA1 deficiency-induced non-canonical pyroptosis priming in podocytes in our system.

**Reducing ability of APE1 mediates IRF1 upregulation in ABCA1 KD podocytes.** In addition to its role in reverse cholesterol transport, ABCA1 also has a role in exporting APE1<sup>7</sup>. APE1, also known as Ref-1 has two functions<sup>20</sup>. First, APE1 reduces transcription factors to activation form and oxidizes itself. Among the transcription factors reduced by APE1 are HIF1 $\alpha$ , NF $\kappa$ B, STAT3, AP1 and p53<sup>21</sup>. Second, APE1 works as an

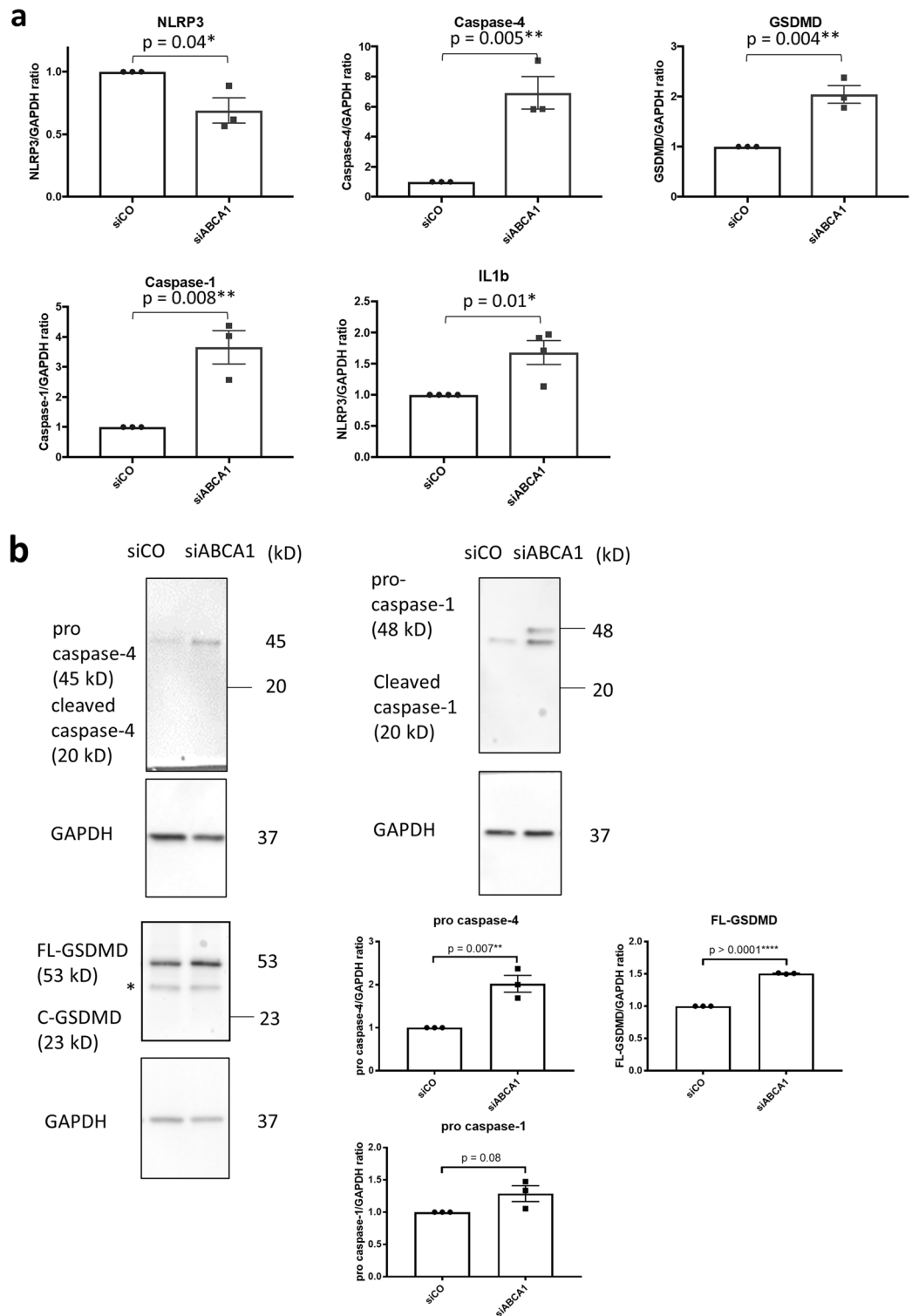


**Figure 1.** mRNA expression and uncleaved protein levels of non-canonical pyroptosis-related genes are increased in siABCA1 podocytes. **(a)** mRNA levels of non-canonical pyroptosis-related genes in siCO and siABCA1 podocytes. **(b)** Protein levels of uncleaved or pro- form of non-canonical pyroptosis-related genes in siCO and siABCA1 podocytes. The bands indicated with \* (around 35 kD) in the FL-GSDMD blot are nonspecific bands. The uncropped blots are in the Supplementary Fig. S1a–c. **(c)** Protein levels of pro-IL1b in cell lysates and supernatants of siCO and siABCA1 podocytes. N = 3 for each group except for IL1β mRNA, which is N = 4. The uncropped blots are in the Supplementary Fig. S1a,d.

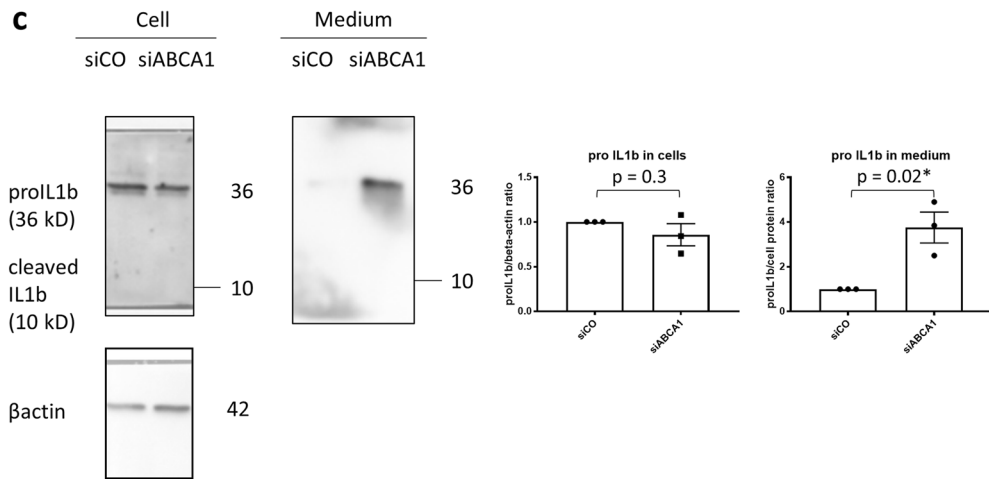


**Figure 1.** (continued)

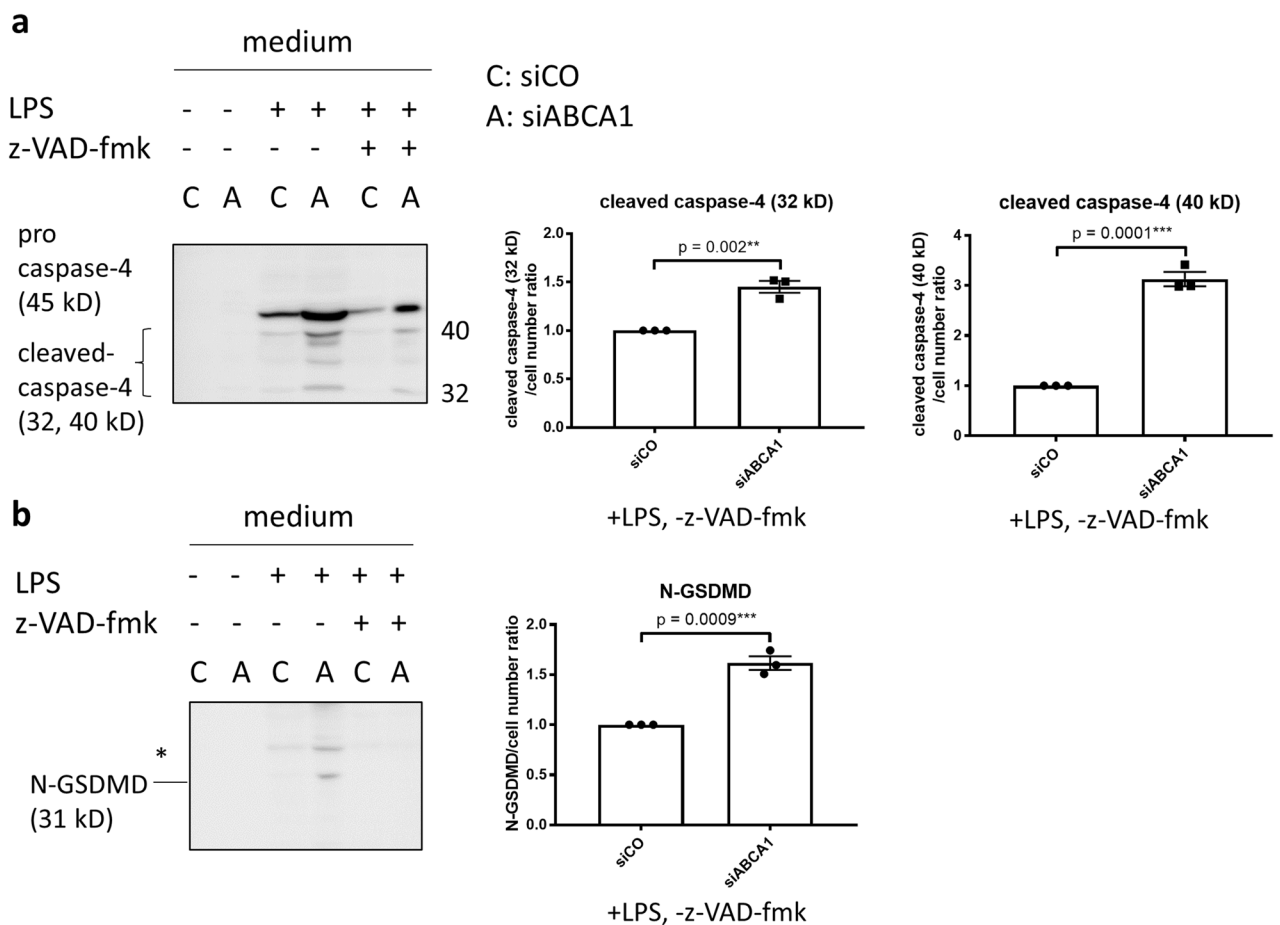


**Figure 2.** Protein levels of cleaved caspase-4 and N-GSDMD activated by LPS electroporation are increased in siABCA1 podocytes. (a) Protein levels of cleaved caspase-4 in siCO and siABCA1 podocytes. (b) Protein levels of N-GSDMD in siCO and siABCA1 podocytes. The uncropped blots are in the Supplementary Fig. S2a,b. N = 3 for each group. Each lane contains medium from the same cell number.

apurinic/apryrimidinic endonuclease to nick the abasic site of DNA to prep it for repair. To examine the amount of APE1 in whole cell and nuclei where it functions, we conducted Western blotting for APE1 in whole cell lysate and nuclear fractions of control and siABCA1 podocytes and found that APE1 was increased in siABCA1 podocytes compared to control both in whole cell lysate and nuclear fractions (Fig. 5a,b). Next, we used APX3330, a specific-inhibitor of oxidation–reduction function of APE1, to address the question if the reduction of transcription factors by APE1 contributes to the priming of non-canonical pyroptosis in siABCA1 podocytes. The APE1

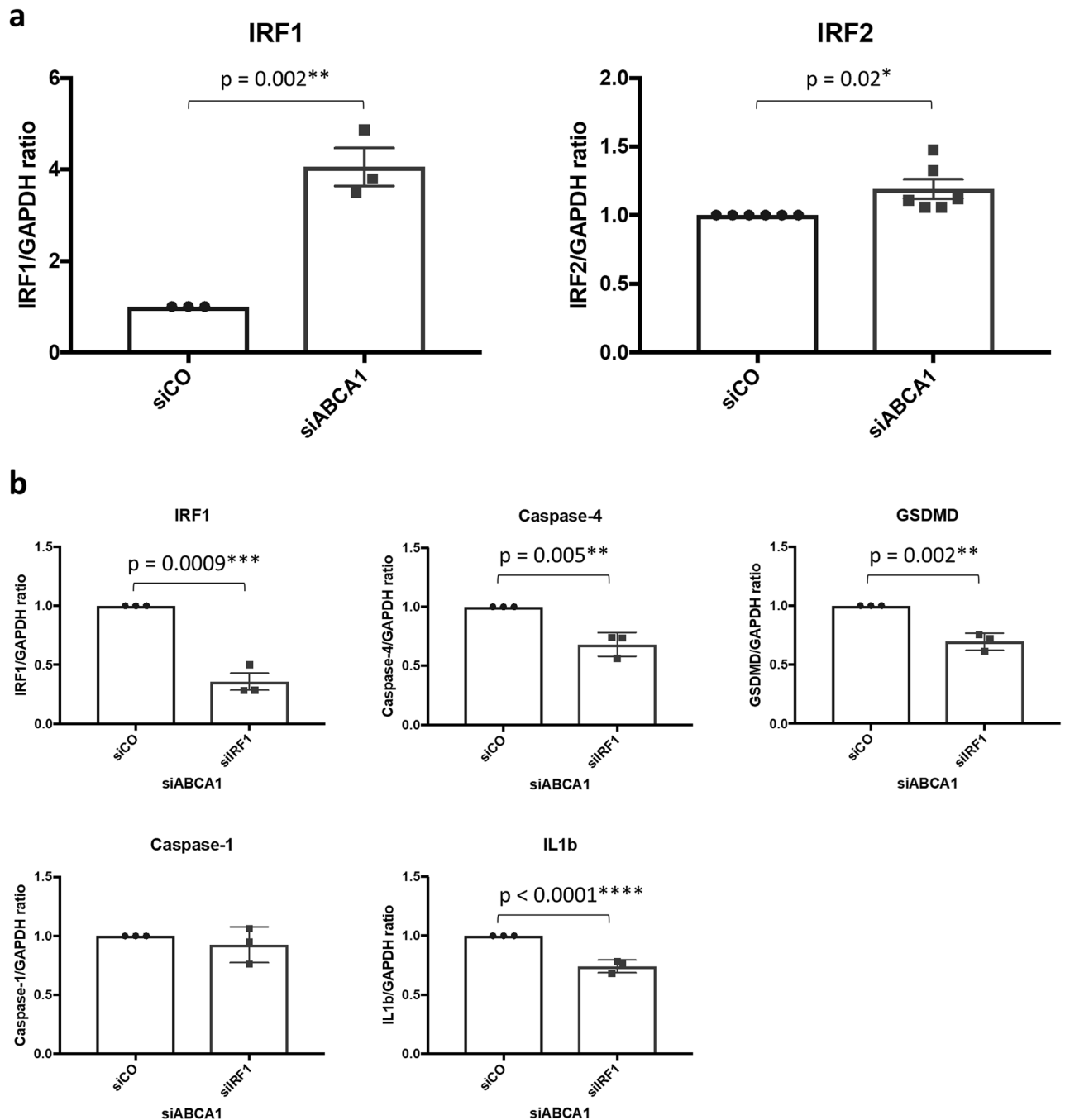


**Figure 3.** IRF1 regulates non-canonical pyroptosis-related genes in siABCA podocytes. **(a)** mRNA levels of IRFs in siCO and siABCA1 podocytes. **(b)** mRNA levels of non-canonical pyroptosis-related genes in siABCA1 podocytes transiently transfected with siCO and siIRF1.  $N = 3$  for each group except for IRF2, which is  $N = 6$ .

redox inhibitor offset the increase of siABCA1-induced mRNA transcription of IRF1 and caspase-4, suggesting a role for APE1 in this process (Fig. 5c).

**NF $\kappa$ B is involved in IRF1 upregulation induced by ABCA1 downregulation.** NF $\kappa$ B is a transcription factor that plays an important role in pyroptosis priming<sup>9</sup>. Several signaling pathways activate NF $\kappa$ B, including reactive oxygen species or TLR4 signaling<sup>22–24</sup>. NF $\kappa$ B can directly induce IRF1 transcription in immune cells while IRF1 can indirectly affect the regulation of NF $\kappa$ B<sup>25,26</sup>. To investigate whether NF $\kappa$ B is involved in the upregulation of IRF1 in siABCA1 podocytes, we used siRNA knockdown for RELA, the NF $\kappa$ B p65 subunit, in siCO and siABCA1 podocytes (Fig. 5d). We found a significant statistical interaction with siABCA1 and siRELA in IRF1 and caspase-4 ( $p_{int} = 0.02$  for IRF1 and 0.006 for caspase-4), which indicated the role of NF $\kappa$ B in siABCA1-induced upregulation of IRF1 and caspase-4 (Fig. 5e). However, we were unable to confirm that the binding of NF $\kappa$ B to binding sites in IRF1 was increased with siABCA1 podocytes (Fig. 5f).

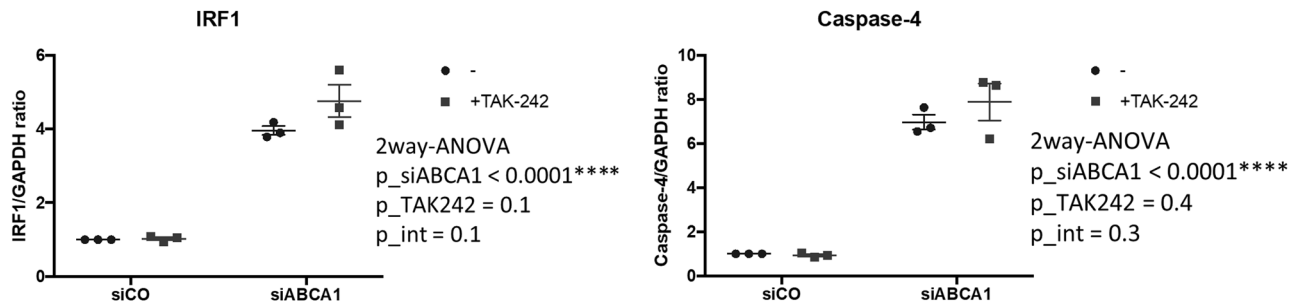


**Figure 4.** TLR4 is not involved in the regulation of IRF1 or caspase-4. mRNA levels of IRF1 and caspase-4 in siCO and siABCA1 cells treated with TAK-242 (TLR4 inhibitor). N = 3 for each group.

**APE1, IRF1 and caspase-11 are increased in glomeruli of BTBR ob/ob mice.** Finally, to investigate whether our in vitro observations translate in vivo, we used BTBR ob/ob mice, a mouse model of DKD. We previously demonstrated that decreased ABCA1 expression in podocytes plays an important role in DKD progression<sup>5,6</sup>. Immunofluorescence staining demonstrated increased APE1 expression in glomeruli of BTBR ob/ob compared to WT mice (Fig. 6a). In support, we found increased mRNA levels of IRF1 and caspase-11, which is compatible with the activation of the ABCA1/APE1/IRF1 axis in vivo as well as in vitro in DKD (Fig. 6b).

## Discussion

In this study, we demonstrated that ABCA1 deficiency in podocytes, which we previously showed to contribute to the progression of DKD, induced non-canonical pyroptosis priming in association with nuclear APE1 accumulation and subsequent activation of transcription factors by redox reaction (Fig. 7). Among the non-canonical pyroptosis-related genes upregulated in siABCA1 podocytes, caspase-4/11, GSDMD and IL1 $\beta$  were identified to be regulated by IRF1, while caspase-1 was not regulated by IRF1 but increased by APE1 redox reaction.

Although the function of ABCA1 has been largely attributed to cholesterol efflux, ABCA1 is also involved in other cellular export mechanisms<sup>27</sup>. ABCA1 participates in the secretion of phospholipids such as cardiolipin, lysophosphatidylcholine and phosphatidylserine, extracellular vesicles and proteins associated with anti-inflammatory response and apoptotic cell clearance<sup>28–31</sup>. Recently, a role for ABCA1 in APE1 export has been described<sup>7</sup>.

APE1 mainly has two functions, an endonuclease and a redox function<sup>20,32</sup>. In its redox function, APE1 is oxidized and a transcription factor is reduced through a thiol/sulfide exchange and activated by facilitated DNA binding. Those transcription factors include NF $\kappa$ B, Hypoxia Inducible Factor (HIF), Signal Transducer and Activator of Transcription 3 (STAT3), Activator Protein 1 (AP-1) and cAMP-response element binding protein (CREB). So far, in canonical and non-canonical pyroptosis priming, NF $\kappa$ B was shown to be activated via phosphorylation of inhibitor of NF $\kappa$ B (I $\kappa$ B) kinases by TLR4 signaling<sup>22,33,34</sup>. The canonical pyroptosis pathway involving NLRP3 contributes to DKD but a contribution of non-canonical pyroptosis was also recently reported<sup>11,35</sup>. This study demonstrates that ABCA1 deficiency in podocytes, which we previously demonstrated to play an important role in DKD progression<sup>5,6</sup>, leads to APE1 accumulation and activation of transcription factors by redox reaction of APE1, not by TLR4, in the absence of NLRP3 increase. Thus, this pathway could represent a new mechanism of non-canonical pyroptosis priming in DKD. Our data suggest that APE1 activates several transcription factors and that the combination of their activation could lead to a distinct pattern of gene expression in siABCA1 podocytes. However, further investigation to elucidate the exact details of this process are warranted. It can also be speculated that the involvement of APE1 in mitochondrial function via the regulation of mitochondrial RNA may contribute to DKD<sup>32</sup>.

Priming of pyroptosis in the absence of an activation or cleavage of pyroptosis-related proteins occurred in siABCA1 podocytes, consistent with our previous observation in vitro and in vivo that ABCA1 downregulation itself is not sufficient to cause injury<sup>6</sup>. Nevertheless, ABCA1 induction has been explored as a treatment for DKD<sup>36</sup>. APE1 has been investigated as a treatment target of malignancy, ocular diseases and inflammatory bowel disease<sup>20,32</sup>, and this study indicates the possibility that it could be a target of DKD as well as IRF1.

We have previously published that oxidized cardiolipin is suggested to be implicated in the sensitization of siABCA1 podocytes to DKD.<sup>6</sup> Some relationship between oxidized phospholipids (oxPLs) and non-canonical pyroptosis are described so far. Oxidized 1-palmitoyl-2-arachidonoyl-*sn*-glycero-3-phosphorylcholine (oxPAPC) can bind caspase-11 and activate it like LPS<sup>37</sup>. On the other hand, although we do not know specifically whether oxidized cardiolipin induces pyroptosis, some other oxPLs are demonstrated to sensitize bone marrow-derived macrophages to N-GSDMD-induced cytotoxicity<sup>38</sup>. It is possible that oxPLs and non-canonical pyroptosis mutually affect each other in ABCA1 downregulated podocytes.

In summary, we demonstrated that ABCA1 deficiency in podocytes, which contributes to DKD progression, induces the expression of non-canonical pyroptosis-related genes such as caspase-4/11, GSDMD, caspase-1 and IL1 $\beta$  via nuclear APE1 accumulation and subsequent reduction of transcription factors. Thus, non-canonical pyroptosis priming by ABCA1/APE1/IRF1 axis could represent a novel pathway to be targeted for the treatment of patients with DKD.

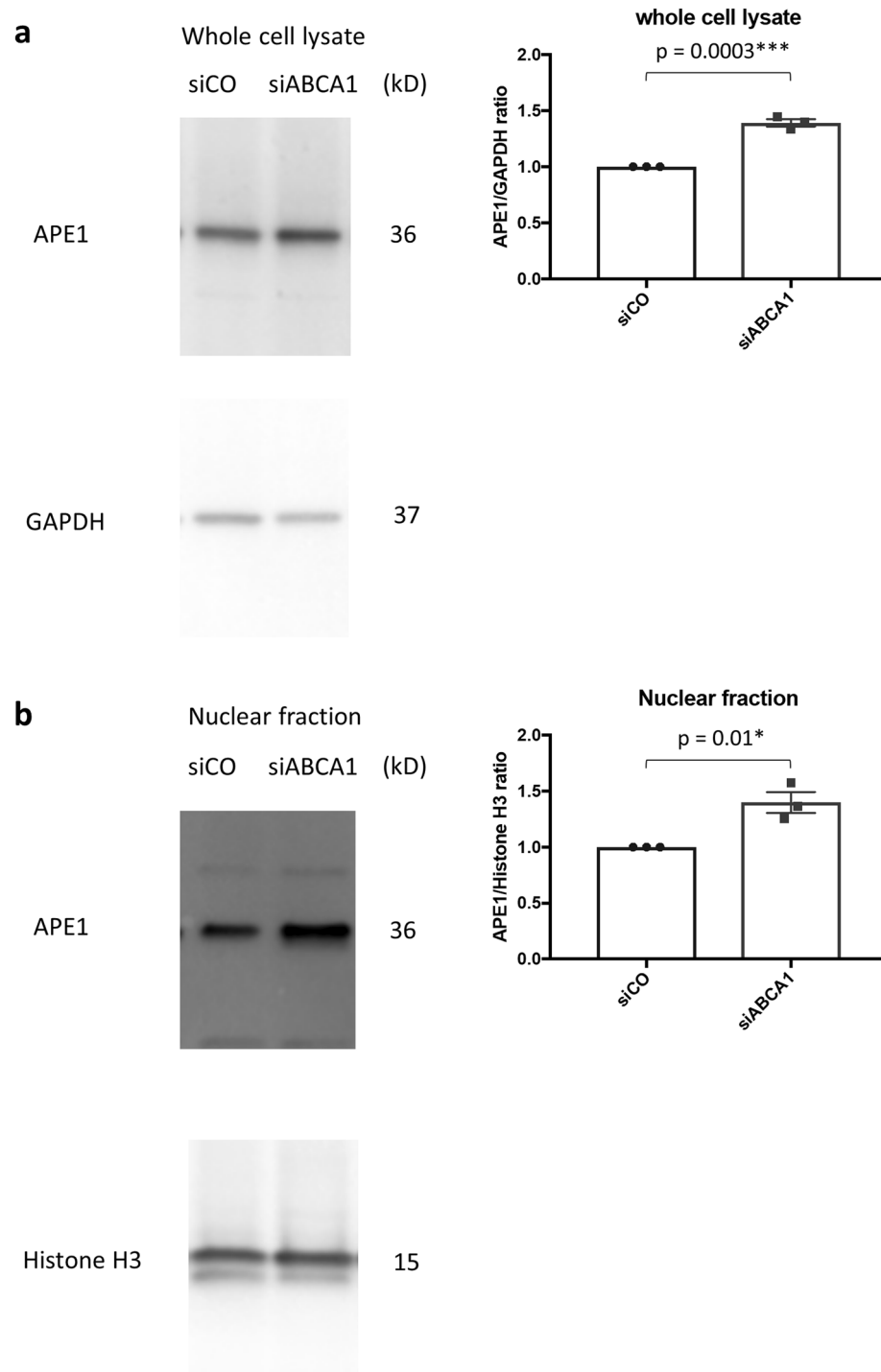


**Figure 5.** APE1 and NF $\kappa$ B regulates the mRNA expression of IRF1 and caspase-4. **(a)** Protein levels of APE1 in whole cell lysate of siCO and siABCA1 podocytes. The uncropped blots are in the Supplementary Fig. S3a. **(b)** Protein levels of APE1 in nuclear fractions of siCO and siABCA1 podocytes. The uncropped blots are in the Supplementary Fig. S3b. **(c)** mRNA levels of IRF1, caspase-4 and caspase-1 in siCO and siABCA1 podocytes treated with DMSO or APX3330 (APE1 redox inhibitor). **(d)** siRELA knockdown efficiency in siCO podocytes.  $N = 3$  for each group. **(e)** mRNA levels of IRF1 and caspase-4 in siABCA1 podocytes transiently transfected with siCO and siRELA. **(f)** The result of ChIP qPCR for siCO podocytes treated with DMSO, siABCA1 podocytes with DMSO and siABCA1 podocytes with APX3330. Neph3 was used as a positive control and HOXA13 as a negative control for NF $\kappa$ B binding to DNA.  $N = 3$  for each group. APE1 apurinic/apyrimidinic endonuclease-1, Neph3 kirre like nephrin family adhesion molecule 2, HOXA13 Homeobox A13.

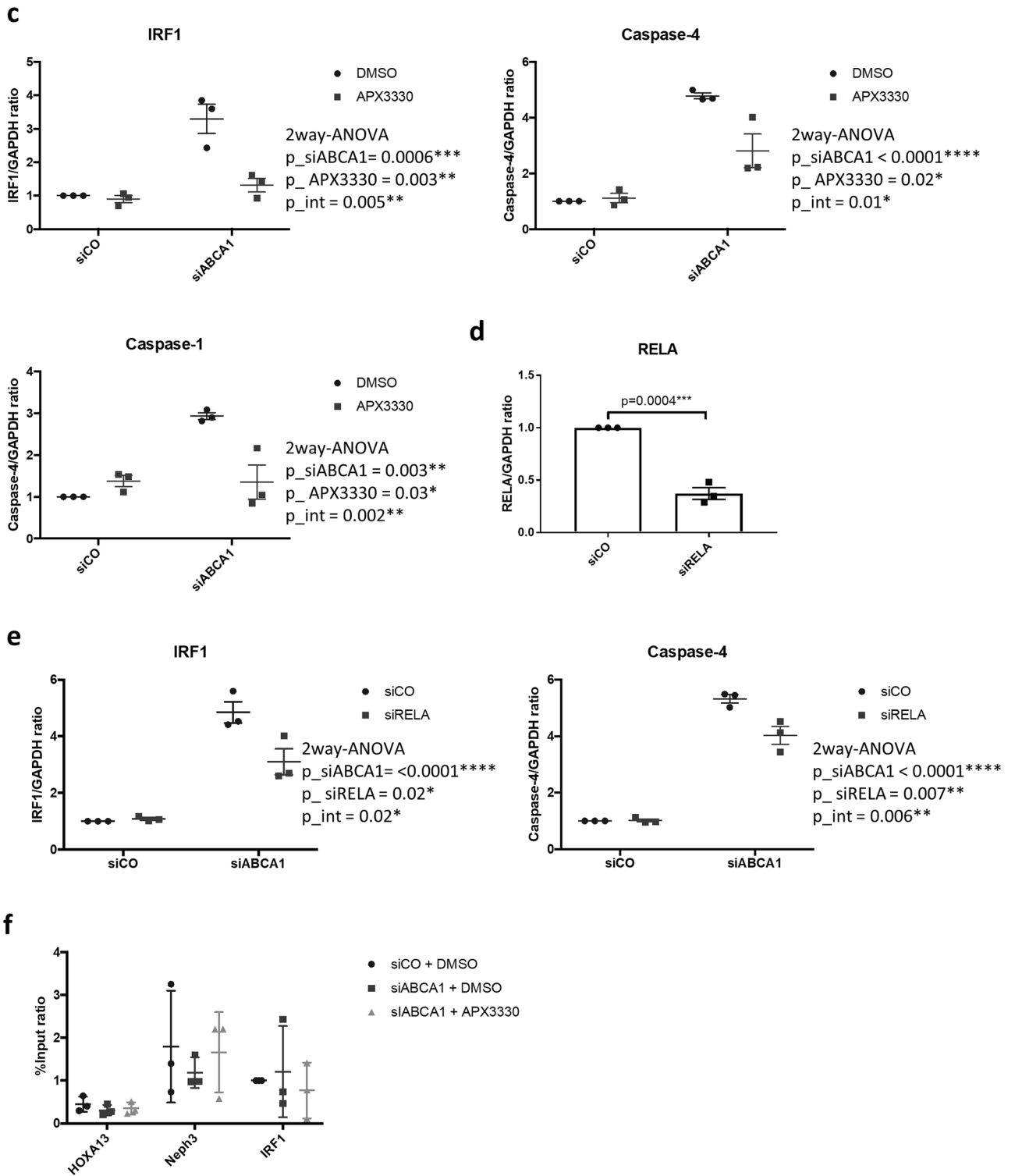
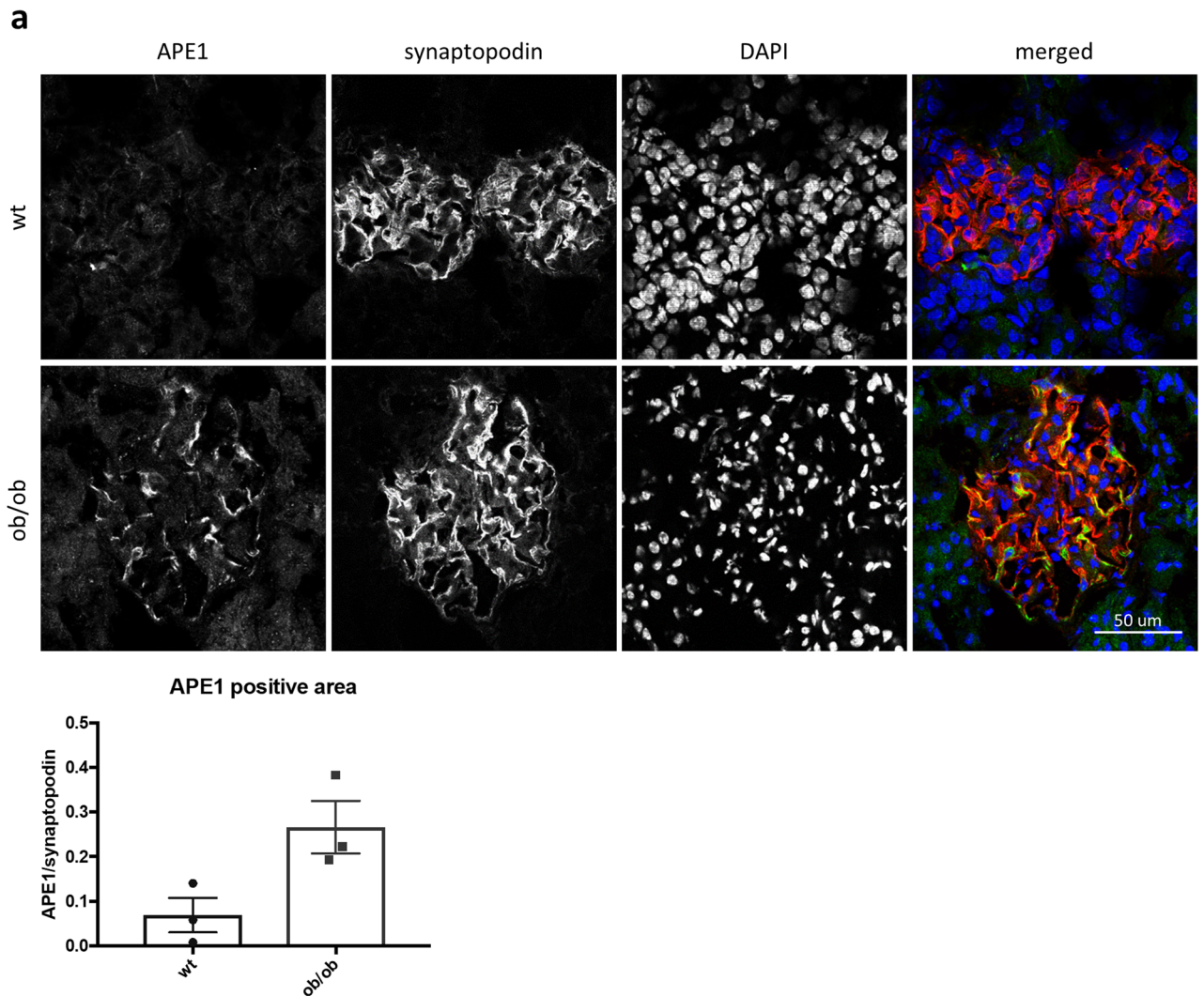


Figure 5. (continued)

### Materials and methods

**Cell culture.** Human podocytes (gift from Dr. Moin Saleem, University of Bristol, Bristol, England) were grown at 33 °C under permissive conditions in RPMI culture medium containing 10% FBS and 1% penicillin/streptomycin and 0.01 mg/ml recombinant human insulin, 0.0055 mg/ml human transferrin (substantially iron-free), and 0.005 µg/ml sodium selenite<sup>39</sup>. Human podocytes were then thermoshifted and differentiated for 14 days at 37 °C in RPMI medium 10% FBS and 1% penicillin/streptomycin. ABCA1 siRNA knockdown (siABCA1) and non-targeting siRNA control (siCO) podocytes were generated and validated as previously described<sup>40</sup>. On day 10–14 of differentiation, podocytes were collected and analyzed. For APE1 inhibition,





**Figure 6.** APE1, IRF1 and non-canonical pyroptosis-related genes are increased in glomeruli of ob/ob mice. **(a)** Representative images of immunofluorescence staining for APE1 (green), synaptopodin (red) and nuclei (blue) in kidney tissue sections of wt and BTBR ob/ob mice and average APE1 positive area/synaptopodin positive area of 10 glomeruli in each mouse. N = 3 for each group. **(b)** mRNA levels of IRF1 and non-canonical pyroptosis-related genes in wt and ob/ob mouse glomeruli. Caspase-11 is the mouse ortholog of caspase-4 in human. N = 9 for each group except for caspase-1 and IL1 $\beta$  in ob/ob, which is n = 8.

podocytes were treated with 1  $\mu$ M TAK-242 (Milipore Sigma, St. Louis MO, USA) for 24 h or 75  $\mu$ M APX3330 (NOVUS biologicals, Centennial, CO, USA) for 48 h.

**Animals.** All animal studies were approved by the Institutional Animal Care and Use Committee (IACUC) at the University of Miami. All experiments were performed in accordance with the guidelines and regulations of IACUC at the University of Miami. Mice were sacrificed at 20 weeks by isoflurane inhalation. The authors complied with the ARRIVE guidelines. All the samples used for this manuscript including mRNA of glomeruli and frozen sections of kidneys of wildtype (wt) and BTBR ob/ob mice were collected and stored for our previous paper<sup>6</sup> and were newly analyzed. The detailed methods are described previously<sup>6</sup>. 9 mice (5 females and 4 males) each were included in wt and ob/ob group. For immunofluorescence, 3 mice from each group which show typical pathological findings of normal or diabetic kidney disease in paraffin sections were selected and tissue in OCT from those 6 mice were freshly cut and analyzed. For qPCR, all the samples were analyzed, but because of the shortage of one sample, only 8 samples were analyzed for caspase-1 and IL1 $\beta$  in ob/ob group.

**siRNA transfection.** We used commercial siRNAs against human IRF1 (Silencer Select, s7501, s7503, Life Technologies Corporation, Carlsbad, CA, USA), RELA (Silencer Select, s11914, Life Technologies Corporation, Carlsbad, CA, USA) and a negative control siRNA (SIC001, Milipore Sigma, St. Louis MO, USA and Silencer Select#1, Life Technologies Corporation, Carlsbad, CA, USA). These siRNAs were introduced into podocytes using HiPerfect (QIAGEN, Hilden, Germany) according to the manufacturer's instructions.

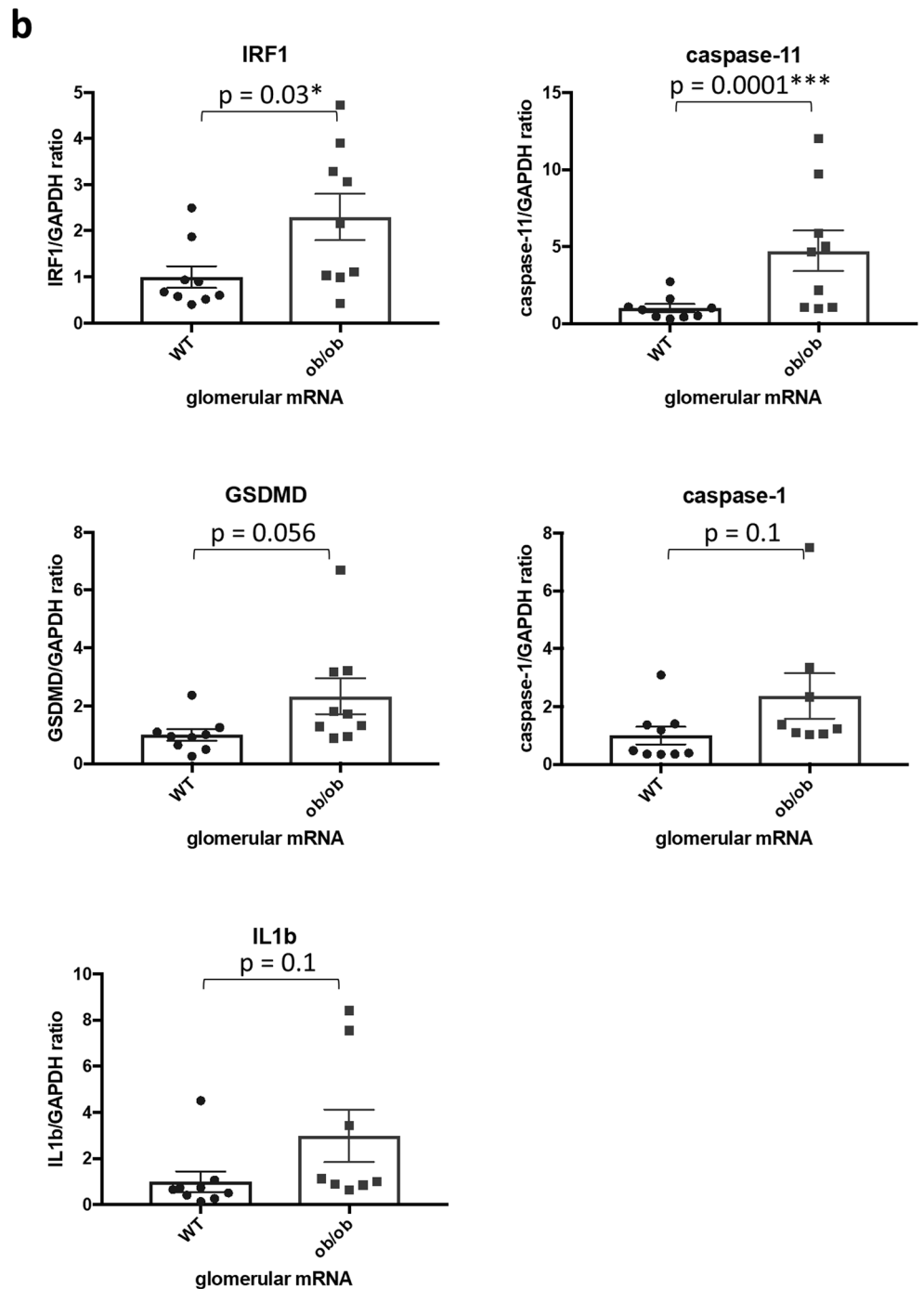


**Figure 6.** (continued)

**Real-time quantitative PCR (qPCR).** Cell RNA was isolated with RNeasy Plus Mini Kit (QIAGEN, Hilden, Germany) and reverse transcribed using qScript DNA SuperMix (Quantabio, Beverly, MA, USA). PCR was performed on a StepOnePlus system (Applied Biosystems, Waltham, MA, USA) with PerfeCTa SYBER Green SuperMix (Quantabio, Beverly, MA, USA). The data were normalized to GAPDH. Primer sequences are listed in Table 1. We repeated at least 3 transient transfections in siRNA KD. Each point per group represents a different transfection of cells. For IL1b mRNA expression and IRF2 mRNA expression we repeated the experiment 4 or 6 times respectively to reach statistical significance because of wide standard deviation.

**Western blotting.** Cells lysates were prepared using RIPA buffer. Protein concentration was measured with the bicinchoninic acid (BCA) reagent (Thermo Fisher Scientific Inc., Waltham, MA, USA). 20–30 µg of protein extract was loaded onto 4 to 20% SDS–polyacrylamide gel electrophoresis (SDS–PAGE) gels (Bio-Rad Laboratories Inc., Hercules, A, USA) and transferred to Immobilon-P PVDF membranes (Bio-Rad Laboratories Inc.,

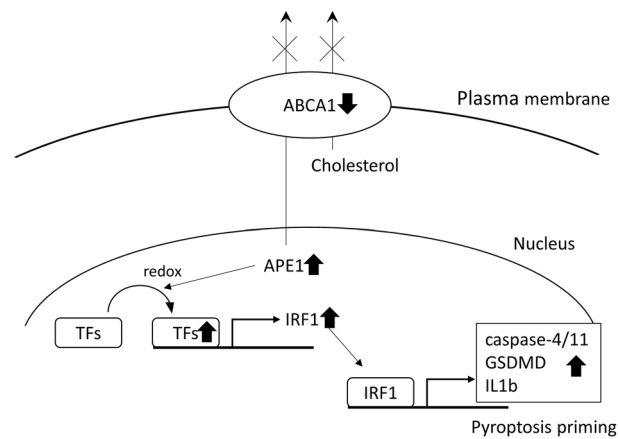


**Figure 7.** Schematic of the hypothesis. ABCA1 deficiency in DKD causes accumulation of APE1 in nuclei, which activates transcription factors including NFκB via redox reaction. Activated transcription factors (TFs) increases IRF1 expression and IRF1 subsequently increases the expression of non-canonical pyroptosis-related genes such as caspase-4/11, GSDMD and IL1β. TFs: transcription factors.

Gene	Use	Species		Sequence
Caspase-4	RT-PCR	Human	Forward	AGATGCCCTCAAGCTTTGTC
			Reverse	TGCGGTTGTTCTCTCCTTT
GSDMD	RT-PCR	Human	Forward	GCCTCCACAACCTCTCTGACAGATG
			Reverse	GGTCTCCACCTCTGCCCGTAG
Caspase-1	RT-PCR	Human	Forward	CACACCGCCCAGAGCACAAG
			Reverse	TCCCACAAATGCCTTCCGAATAC
IL1b	RT-PCR	Human	Forward	TTCGACACATGGGATAACGAGG
			Reverse	TTTTTGCTGTGAGTCCCGGAG
NLRP3	RT-PCR	Human	Forward	CTTCTCTGATGAGGCCAAG
			Reverse	GCAGCAAACCTGGAAAGGAAG
IRF1	RT-PCR	Human	Forward	CCAGAGCAGGAACAAGGG
			Reverse	GGTCATCAGGCAGAGTGGGA
IRF2	RT-PCR	Human	Forward	TGGATGCATGCGGCTAGA
			Reverse	CATCTGAAATTCGCCTTCC
GAPDH	RT-PCR	Human	Forward	TGCACCACCAACTGCTTAGC
			Reverse	GGCATGGACTGTGGTCATGAG
Caspase-11	RT-PCR	Mouse	Forward	CCTGAAGAGTTCACAAGGCTT
			Reverse	CCTTTCGTGTACGGCCATTG
GSDMD	RT-PCR	Mouse	Forward	CCATCGGCCTTTGAGAAAGTG
			Reverse	ACACATGAATAACGGGGTTTCC
Caspase-1	RT-PCR	Mouse	Forward	AATGAAGTTGCTGCTGGAGGA
			Reverse	CAGAAGTCTGTGCTCTGGGC
IL1b	RT-PCR	Mouse	Forward	GCAACTGTTCTGAACTCAACT
			Reverse	ATCTTTGGGGTCCGTCAACT
IRF1	RT-PCR	Mouse	Forward	CTTCGTCGAGGTAGGACGTG
			Reverse	CTTTGCTGCAGGAGCGATTC
GAPDH	RT-PCR	Mouse	Forward	GAAGGGCTCATGACCACA
			Reverse	GGATGCAGGGATGATGTTCT
HOXA13	ChIP	Human	Forward	GCTTCTTCTCCCTCCTA
			Reverse	CCGATCCCTGTGTAACCTGC
Neph3	ChIP	Human	Forward	GAGTTTCTCAACGGGAAGAG
			Reverse	GCCTCTGACGCTCTGAAAC
IRF1	ChIP	Human	Forward	CCACCGAGCAATCCAAACAC
			Reverse	GCCTGATTCCCCGAAATGAC

**Table 1.** Primers used in the article. Sequences of the primers used for RT-PCR and ChIP in the article.

Hercules, A, USA). Western blot analysis was performed using following primary antibodies: caspase-4 (\$4450, rabbit, 1:1000), caspase-1 (#3866, rabbit, 1:1000 all from Cell Signaling Technology Inc.), IL1 $\beta$  (AF-201-NA, goat, 1:1000, R and D systems), GSDMD (ab210070, rabbit, 1:1000, Abcam PLC), N-GSDMD (ab215203, rabbit, 1:1000, Abcam PLC), APE1 (NB100-116, mouse, 1:1000, NOVUS biologicals), GAPDH (CB1001, mouse, 1:10,000, Sigma-Aldrich), beta actin (A3854, mouse, 1:10,000, Sigma-Aldrich); or secondary antibodies: anti-mouse IgG HRP (Promega, W402B, 1:10,000), anti-rabbit IgG HRP (Promega, W401B, 1:10,000), anti-goat IgG HRP (Promega, V8051, 1:10,000). Signal was detected with Radiance ECL (Azure Biosystems Inc., Dublin, CA, USA) or WesternBright ECL (Advansta Inc., San Jose, CA, USA) using Azure c600 Imaging System.

Protein from supernatants were isolated using Spin-X UF Concentrator (Corning Inc., Corning, NY, USA) and the values were normalized to the protein concentration of cells in the medium.

Nuclear fractions were obtained using a Cell Fractionation Kit (ab109719, Abcam PLC, Cambridge, UK) according to the manufacturer's instructions.

**LPS electroporation.** LPS was electroporated into podocytes using program T-020 in Nucleofector 2b (Lonza, Valais, Switzerland) and Amexa Basic Nucleofector Kit for Primary Mammalian epithelial cells (VPI-1005) according to manufacturer's instruction. LPS-EB ultrapure (Invivogen, San Diego, CA, USA) was added to differentiated podocytes at a concentration of 3.0 ng/400,000 cells. The supernatants were collected at 4 h after electroporation and protein from them were collected using Amicon Ultra (Merck, Darmstadt, Germany) and analyzed with western blotting. Samples were normalized to mL/number of cells in the medium. Z-VAD-fmk (Selleck Biotech, Tokyo, Japan) was added 1 h prior to, during and after electroporation at a concentration of 20 nM.

**Chromatin Immunoprecipitation (ChIP).** The binding of NF $\kappa$ B to the IRF1 promoter was assessed using the chromatin immunoprecipitation assay. Podocytes were cross-linked for 10 min using 1% paraformaldehyde and sonicated into fragments. The fragmented DNA forming a complex with NF $\kappa$ B was immunoprecipitated with an anti-NF $\kappa$ B rabbit polyclonal antibody (Cell Signaling Technology, Inc. Danvers, MA, USA) and Dynabeads M-280 Sheep Anti-Rabbit IgG (Invitrogen, St. Louis MO, USA). The precipitated DNA was used as a template for PCR reactions with the primers listed in Table 1. Five NF $\kappa$ B binding sites in IRF promoter region (-500 to +1500 from the transcription starting point) were predicted by FIMO database and the one nearest to the transcription starting site was selected, which was consistent with the publicly available ChIP-seq data which showed a strong peak near the transcription starting site in B-lymphocytes (GSM935478, GSM935526, GSM935285, GSM5529, GSM935531, GSM935273 and GSM935279)<sup>25</sup>. Neph3 (also known as kirre like nephrin family adhesion molecule 2) promoter region has known NF $\kappa$ B-binding site, and was used as a positive control<sup>41</sup>. Homeobox A13 (HOXA13) is the negative-control primer, which was designed for the promoter regions of chromosome 20.

**Immunofluorescence.** For immunofluorescence staining of kidneys from mice, fresh cut 4  $\mu$ m-thick tissue in OCT was used. No fixation agent was applied. Permeabilization was performed using 0.3% Triton X-100 in 1  $\times$  PBS for 15 min at room temperature. A blocking step was performed using Power Block Universal Blocking Reagent (BioGenex, Fremont CA, USA) for 10 min at room temperature. Primary antibodies (for APE1 (NB100-101, rabbit, 1:500, NOVUS biologicals) and synaptopodin (sc-21537, goat, 1:500, Santa Cruz Biotechnology Inc.) were used for 24 h at 4  $^{\circ}$ C. Secondary antibodies (anti-rabbit Alexa Flour 488 (A32790, donkey, Invitrogen) and anti-goat Alexa Flour 568 (A11057, donkey, Invitrogen)) were used for 1 h at room temperature. The anti-caspase-11 antibody was conjugated with Alexa Flour 594 and used without secondary antibodies. To detect nucleus, ProLong Gold antifade reagent with DAPI (Invitrogen, St. Louis MO, USA) was applied.

Images were acquired by laser scanning confocal microscopy using a Leica SP5 Inverted microscope,  $\times$ 20 objective (Leica Microsystems CMS GmbH, Germany). Measuring of cell fluorescence was performed using Image J software.

**Statistical analysis.** All the data are reported as mean  $\pm$  standard error of mean and as individual values in the dot plots. Two groups were compared using independent sample t-test and a two-way ANOVA test was used to analyze the effect of two independent factors on outcomes and investigate if there is an interaction effect between the two factors on the outcomes. A p-value < 0.05 was considered statistically significant for all tests. GraphPad Prism, version 7.0 (GraphPad Software Inc., San Diego, CA, USA) was used for data analyses.

## Data availability

The data underlying this article are available in the article. The datasets referred to in the current study are available in the the Gene Expression Omnibus (GEO) repository, GSM935478, GSM935526, GSM935285, GSM5529, GSM935531, GSM935273 and GSM935279.

Received: 15 December 2022; Accepted: 18 May 2023

Published online: 14 June 2023

## References

- Murray, C. J. L. & Lopez, A. D. Measuring the global burden of disease. *N. Engl. J. Med.* **369**, 448–457 (2013).
- González-Pérez, A., Saez, M., Vizcaya, D., Lind, M. & García Rodríguez, L. Incidence and risk factors for mortality and end-stage renal disease in people with type 2 diabetes and diabetic kidney disease: A population-based cohort study in the UK. *BMJ Open Diabetes Res. Care* **9**, e002146 (2021).

3. Meyer, T. W., Bennett, P. H. & Nelson, R. G. Podocyte number predicts long-term urinary albumin excretion in Pima Indians with Type II diabetes and microalbuminuria. *Diabetologia* **42**, 1341–1344 (1999).
4. Wiggins, J. E. *et al.* Podocyte hypertrophy, 'adaptation', and 'decompensation' associated with glomerular enlargement and glomerulosclerosis in the aging rat: Prevention by calorie restriction. *J. Am. Soc. Nephrol.* **16**, 2953–2966 (2005).
5. Merscher-Gomez, S. *et al.* Cyclodextrin protects podocytes in diabetic kidney disease. *Diabetes* **62**, 3817–3827 (2013).
6. Ducasa, G. M. *et al.* ATP-binding cassette A1 deficiency causes cardiolipin-driven mitochondrial dysfunction in podocytes. *J. Clin. Invest.* **130**, 3387–3400 (2019).
7. Lee, Y. R. *et al.* ATP binding cassette transporter A1 is involved in extracellular secretion of acetylated APE1/Ref-1. *Int. J. Mol. Sci.* **20**, 3178 (2019).
8. Shahzad, K. *et al.* Nlrp3-inflammasome activation in non-myeloid-derived cells aggravates diabetic nephropathy. *Kidney Int.* **87**, 74–84 (2015).
9. Swanson, K. V., Deng, M. & Ting, J. P. Y. The NLRP3 inflammasome: Molecular activation and regulation to therapeutics. *Nat. Rev. Immunol.* **19**, 477–489 (2019).
10. Downs, K. P., Nguyen, H., Dorfleutner, A. & Stehlik, C. An overview of the non-canonical inflammasome. *Mol. Aspects Med.* **76**, 100924 (2020).
11. Cheng, Q. *et al.* Caspase-11/4 and gasdermin D-mediated pyroptosis contributes to podocyte injury in mouse diabetic nephropathy. *Acta Pharmacol. Sin.* **42**, 954–963 (2021).
12. Wang, Y. *et al.* TLR4/NF- $\kappa$ B signaling induces GSDMD-related pyroptosis in tubular cells in diabetic kidney disease. *Front. Endocrinol.* **10**, 603 (2019).
13. Yu, Q., Zhang, M., Qian, L., Wen, D. & Wu, G. Luteolin attenuates high glucose-induced podocyte injury via suppressing NLRP3 inflammasome pathway. *Life Sci.* **225**, 1–7 (2019).
14. Santos, J. C. *et al.* Human GBP1 binds LPS to initiate assembly of a caspase-4 activating platform on cytosolic bacteria. *Nat. Commun.* **11**, 1–15 (2020).
15. Wang, K. *et al.* Structural mechanism for GSDMD targeting by autoprocessed caspases in pyroptosis. *Cell* **180**, 941–955.e20 (2020).
16. Benaoudia, S. *et al.* A genome-wide screen identifies IRF2 as a key regulator of caspase-4 in human cells. *EMBO Rep.* **20**, e48235 (2019).
17. Kayagaki, N. *et al.* IRF2 transcriptionally induces GSDMD expression for pyroptosis. *Sci. Signal.* **12**, 4917 (2019).
18. Thygesen, S. J. & Katryn, S. J. IRF1 and IRF2 regulate the non-canonical inflammasome. *EMBO Rep.* **20**, e48891 (2019).
19. Zhu, X. *et al.* Macrophage ABCA1 reduces MyD88-dependent Toll-like receptor trafficking to lipid rafts by reduction of lipid raft cholesterol. *J. Lipid Res.* **51**, 3196–3206 (2010).
20. Shah, F. *et al.* Exploiting the Ref-1-APE1 node in cancer signaling and other diseases: From bench to clinic. *NPJ Precis. Oncol.* **1**, 19 (2017).
21. Hartman, G. D., Lambert-Cheatham, N. A., Kelley, M. R. & Corson, T. W. Inhibition of ape1/ref-1 for neovascular eye diseases: From biology to therapy. *Int. J. Mol. Sci.* **22**, 10279 (2021).
22. Rathinam, V. A. K. *et al.* TRIF licenses caspase-11-dependent NLRP3 inflammasome activation by gram-negative bacteria. *Cell* **150**, 606–619 (2012).
23. Lin, J. *et al.* New insights into the mechanisms of pyroptosis and implications for diabetic kidney disease. *Int. J. Mol. Sci.* **21**, 1–23 (2020).
24. Yang, X., Wang, Y. & Gao, G. High glucose induces rat mesangial cells proliferation and MCP-1 expression via ROS-mediated activation of NF- $\kappa$ B pathway, which is inhibited by eleutheroside E. *J. Recept. Signal Transduct. Res.* **36**, 152–157 (2016).
25. Iwanaszko, M. & Kimmel, M. NF- $\kappa$ B and IRF pathways: Cross-regulation on target genes promoter level. *BMC Genom.* **16**, 307 (2015).
26. Ghislat, G. *et al.* NF- $\kappa$ B-dependent IRF1 activation programs cDC1 dendritic cells to drive antitumor immunity. *Sci. Immunol.* **6**, 3570 (2021).
27. Chen, W., Wang, S. & Xing, D. New horizons for the roles and association of APE1/Ref-1 and ABCA1 in atherosclerosis. *J. Inflamm. Res.* **14**, 5251–5271 (2021).
28. Shen, X., Zhang, S., Guo, Z., Xing, D. & Chen, W. The crosstalk of ABCA1 and ANXA1: A potential mechanism for protection against atherosclerosis. *Mol. Med.* **26**, 1–8 (2020).
29. Hafiane, A. & Genest, J. ATP binding cassette A1 (ABCA1) mediates microparticle formation during high-density lipoprotein (HDL) biogenesis. *Atherosclerosis* **257**, 90–99 (2017).
30. Hamon, Y. *et al.* ABC1 promotes engulfment of apoptotic cells and transbilayer redistribution of phosphatidylserine. *Nat. Cell Biol.* **2**, 399–406 (2000).
31. Morizawa, Y. M. *et al.* Reactive astrocytes function as phagocytes after brain ischemia via ABCA1-mediated pathway. *Nat. Commun.* **8**, 28 (2017).
32. Caston, R. A. *et al.* The multifunctional APE1 DNA repair–redox signaling protein as a drug target in human disease. *Drug Discov. Today* **26**, 218–228 (2021).
33. Schauvliege, R., Vanrobaeys, J., Schotte, P. & Beyaert, R. Caspase-11 gene expression in response to lipopolysaccharide and interferon-gamma requires nuclear factor-kappa B and signal transducer and activator of transcription (STAT) 1. *J. Biol. Chem.* **277**, 41624–41630 (2002).
34. Yu, H., Lin, L., Zhang, Z., Zhang, H. & Hu, H. Targeting NF- $\kappa$ B pathway for the therapy of diseases: Mechanism and clinical study. *Signal Transduct. Target. Ther.* **5**, 312 (2020).
35. Hou, Y. *et al.* NLRP3 inflammasome negatively regulates podocyte autophagy in diabetic nephropathy. *Biochem. Biophys. Res. Commun.* **521**, 791–798 (2020).
36. Wright, M. B. *et al.* Compounds targeting OSBPL7 increase ABCA1-dependent cholesterol efflux preserving kidney function in two models of kidney disease. *Nat. Commun.* **12**, 1–14 (2021).
37. Zanoni, I. *et al.* An endogenous caspase-11 ligand elicits interleukin-1 release from living dendritic cells. *Science* **352**, 1232–1236 (2016).
38. Kang, R. *et al.* Lipid peroxidation drives gasdermin D-mediated pyroptosis in lethal polymicrobial sepsis. *Cell Host Microbe* **24**, 97–108.e4 (2018).
39. Saleem, M. A. *et al.* A conditionally immortalized human podocyte cell line demonstrating nephrin and podocin expression. *J. Am. Soc. Nephrol.* **13**, 630–638 (2002).
40. Pedigo, C. E. *et al.* Local TNF causes NFATc1-dependent cholesterol-mediated podocyte injury. *J. Clin. Invest.* **126**, 3336–3350 (2016).
41. Ristola, M. *et al.* Regulation of Neph3 gene in podocytes: Key roles of transcription factors NF- $\kappa$ B and Sp1. *BMC Mol. Biol.* **10**, 1–12 (2009).

## Acknowledgements

We would like to thank Prof. Masaomi Nangaku for his valuable assistance with ChIP and electroporation experiments. MI draw Fig. 7.

## Author contributions

M.I., S.M. and A.F. conceived and designed the analysis. M.I. collected the data, performed the analysis and wrote the original draft. G.M.D. collected the animal samples. J.D.M., J.V.S., S.K.M., J.J.K., M.G. A.M. and A.S. contributed data. M.I., S.M., I.M. and A.F. reviewed and edited the manuscript. All authors have read and agreed to the published version of the manuscript.

## Funding

M.I. is supported by Manpei Suzuki Diabetes Foundation. A.F. and S.M. are inventors on pending (PCT/US2019/032215; US 17/057,247; PCT/US2019/041730; PCT/US2013/036484; US 17/259,883; US17/259,883; JP501309/2021, EU19834217.2; CN-201980060078.3; CA2,930,119; CA3,012,773; CA2,852,904) or issued patents (US10,183,038 and US10,052,345) aimed at preventing and treating renal disease. They stand to gain royalties from their future commercialization. A.F. is Vice-President of L&F Health LLC and is a consultant for ZyVersa Therapeutics, Inc. ZyVersa Therapeutics, Inc has licensed worldwide rights to develop and commercialize hydroxypropyl-beta-cyclodextrin from L&F Research for the treatment of kidney disease. A.F. also holds equities in Renal 3 River Corporation. S.M. holds indirect equity interest in, and potential royalty from, ZyVersa Therapeutics, Inc. by virtue of assignment and licensure of a patent estate. A.F. and S.M. are supported by Aurinia Pharmaceuticals Inc. Other authors do not possess any conflict of interest.

## Competing interests

M.I. is supported by Manpei Suzuki Diabetes Foundation. A.F. and S.M. are inventors on pending (PCT/US2019/032215; US 17/057,247; PCT/US2019/041730; PCT/US2013/036484; US 17/259,883; US17/259,883; JP501309/2021, EU19834217.2; CN-201980060078.3; CA2,930,119; CA3,012,773; CA2,852,904) or issued patents (US10,183,038 and US10,052,345) aimed at preventing and treating renal disease. They stand to gain royalties from their future commercialization. A.F. is Vice-President of L&F Health LLC and is a consultant for ZyVersa Therapeutics, Inc. ZyVersa Therapeutics, Inc has licensed worldwide rights to develop and commercialize hydroxypropyl-beta-cyclodextrin from L&F Research for the treatment of kidney disease. A.F. also holds equities in Renal 3 River Corporation. S.M. holds indirect equity interest in, and potential royalty from, ZyVersa Therapeutics, Inc. by virtue of assignment and licensure of a patent estate. A.F. and S.M. are supported by Aurinia Pharmaceuticals Inc. Other authors do not possess any conflict of interest.

## Additional information

**Supplementary Information** The online version contains supplementary material available at <https://doi.org/10.1038/s41598-023-35499-5>.

**Correspondence** and requests for materials should be addressed to M.I. or A.F.

**Reprints and permissions information** is available at [www.nature.com/reprints](http://www.nature.com/reprints).

**Publisher's note** Springer Nature remains neutral with regard to jurisdictional claims in published maps and institutional affiliations.



**Open Access** This article is licensed under a Creative Commons Attribution 4.0 International License, which permits use, sharing, adaptation, distribution and reproduction in any medium or format, as long as you give appropriate credit to the original author(s) and the source, provide a link to the Creative Commons licence, and indicate if changes were made. The images or other third party material in this article are included in the article's Creative Commons licence, unless indicated otherwise in a credit line to the material. If material is not included in the article's Creative Commons licence and your intended use is not permitted by statutory regulation or exceeds the permitted use, you will need to obtain permission directly from the copyright holder. To view a copy of this licence, visit <http://creativecommons.org/licenses/by/4.0/>.

© The Author(s) 2023